Aquaculture 558 (2022) 738391

Contents lists available at ScienceDirect

Aquaculture

journal homepage: www.elsevier.com/locate/aquaculture

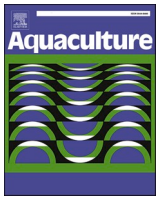

On genome editing in embryos and cells of the freshwater prawn *Macrobrachium rosenbergii*

Jonathan Molcho [a], Rivka Manor [a,b], Maayan Shamsian [a], Gurucharan Sudarshan [a], Rivka Ofir [c,d], Danit Parker [c], Simy Weil [a], Hanin Wattad [a], Emily Hayun [a], Tom Levy [a], Eliahu D. Aflalo [a,e], Ayal Hendel [f], Amir Sagi [a,b,*]

[a] Department of Life Sciences, Ben-Gurion University of the Negev, P.O. Box 653, Beer-Sheva 84105, Israel
[b] The National Institute for Biotechnology in the Negev, Ben-Gurion University of the Negev, P.O. Box 653, Beer-Sheva 84105, Israel
[c] Colors Farm Ltd, Moshav Hazeva 124, Mobile Post Arava, Israel
[d] Dead Sea & Arava Science Center, Central Arava Branch, 8681500, Israel
[e] Department of Life Sciences, Achva Academic College, Mobile Post Shikmim, 7980400, Israel
[f] The Mina and Everard Goodman Faculty of Life Sciences, Advanced Materials and Nanotechnology Institute, Bar-Ilan University, Ramat Gan, Israel

ARTICLE INFO

Keywords:
CRISPR/Cas9
Embryos
Genome editing patterns
Macrobrachium rosenbergii
Primary cell culture
Ribonucleoprotein (RNP)

ABSTRACT

The clustered regularly interspaced short palindromic repeats (CRISPR) technology provides the means for accurate genomic editing. It has been applied in many kinds of cells and animals for functional genomic studies and for precise selective breeding. Nonetheless, this method has not yet been applied in one of the most important – and well studied – decapod crustacean aquaculture species, the giant freshwater prawn *Macrobrachium rosenbergii*. We thus established two CRISPR platforms for *M. rosenbergii*—the first through direct injection into early-stage embryos (entire organism genome editing) and the second by electroporation of a primary embryonic cell culture. The systems were calibrated by optimizing Cas9 concentrations, delivery methods and editing efficiencies. Editing patterns utilizing multiple guides were examined through next generation sequencing. Our results showed a wide range of editing efficiencies in embryos, in some cases reaching as high as 100%. In contrast, in primary embryonic cell cultures, the highest editing efficiency obtained reached a maximum of 64%. In addition, there was a striking difference between the two platforms in terms of the pattern of deletions around the Cas9 cut site. This finding suggests distinct repair mechanisms in the two systems, which calls for further clarification. A phenotypic proof of concept was provided through the investigation of an early acting paired box protein 6 (Pax6) transcription factor, which showed clear effects on eye development in edited embryos and larvae. The current study lays down the foundations for precise functional genomic research and applications of genome editing in crustacean species for both aquaculture and sustainable biocontrol, opening opportunities for the creation of selected crustacean lines with distinct attributes.

1. Introduction

The giant freshwater prawn *Macrobrachium rosenbergii* (Decapoda, Crustacea) is one of the most important species in crustacean aquaculture, but its production volumes have not increased significantly in the past decade (FAO, 2020). Despite several attempts to improve yields through classical selective breeding (Pillai et al., 2020) and efforts to adjust *M. rosenbergii* aquaculture to industrial-sized indoor systems through monosex culture (Levy et al., 2016), there has been no marked improvement to date in yields per area. It is thus evident that other measures of genetic improvement are needed for enhancing yields. A promising minimal-intervention way forward (in contrast to radical genomic modifications through genetic engineering) may lie in a single basepair knock out (KO) through clustered regularly interspaced short palindromic repeats (CRISPR) gene editing.

Particularly when used in concert with a Cas protein (the CRISPR/Cas system), CRISPR editing has become a prominent technique that has found application in the generation of edited organisms and in gene function research (Ceasar et al., 2016). With advances in this system, genome editing of unconventional and non-model research animals is

* Corresponding author at: Department of Life Sciences, Ben-Gurion University of the Negev, P.O. Box 653, Beer-Sheva 84105, Israel.
E-mail address: sagia@bgu.ac.il (A. Sagi).

https://doi.org/10.1016/j.aquaculture.2022.738391
Received 24 February 2022; Received in revised form 18 May 2022; Accepted 19 May 2022
Available online 25 May 2022

now possible. Many applications were theoretically suggested and some have now been implemented in practice in certain fields (Hsu et al., 2014). As part of this trend, the advantages of the CRISPR/Cas implementation have been studied in aquaculture (Gratacap et al., 2019; Okoli et al., 2021), one of the fastest growing commercial food sectors (FAO, 2020), and promising results have been already been obtained for genetically edited fish (Edvardsen et al., 2014; Kim et al., 2019; Kishimoto et al., 2018). Similarly, in cultured crustaceans, which comprise a significant and growing-fast sector of the aquaculture industry (FAO, 2020), initial experiments indicate exciting future prospects (Gui et al., 2016; Kumagai et al., 2017; Martin et al., 2016; Xu et al., 2020) but also a pressing need to establish appropriate tools.

In efforts to develop such tools, one of the primary considerations is that genome editing in animals requires an intervention at early stages of development. This consideration also holds for crustaceans, whose early developmental stages follow the standard oviparous embryonic and larval development path common to most arthropods (Minelli et al., 2016). In *M. rosenbergii*, embryonic development is characterized by a distinctive phenomenon in which the first cell divisions occur only after the first two nuclear divisions (Ling, 1969a). Thus, in the current study, it was this phenomenon that directed the platform for CRISPR editing to early-stage embryos at exactly the same stage(s). Since this 'constraint' is difficult to realize experimentally, we also used an alternative platform based on primary cell cultures, which offers the advantage of higher throughput experimentation vis-à-vis whole animal editing (Ma et al., 2017).

To establish and calibrate the CRISPR system in *M. rosenbergii* for both the above platforms, we looked for a highly expressed gene with a supposedly favorable chromatin architecture to serve as reference. *Actin-depolymerizing factor (ADF)/cofilin*, which was first discovered in porcine brain (Maekawa et al., 1984), appeared to be an appropriate candidate gene for the study. Its translated product is bound to actin and it is involved in actin filament dynamics, indicating that it is essential for eukaryotic cells (Bamburg, 1999). Although no studies have been performed on crustacean *cofilin*, homologs of *cofilin* have been mentioned in transcriptomic and proteomic studies in several crustacean species (Chang et al., 2016; Wu et al., 2009), which suggests that such a gene does indeed exist in the *M. rosenbergii* genome.

Following a study of *cofilin* designed to demonstrate the possibility of Cas9 KO in *M. rosenbergii*, proof of concept for editing with an early clear phenotype was needed. For this purpose, the non-lethal *Paired box protein 6* (*Pax6*), a highly conserved transcription factor that plays a crucial role in early eye development, was selected. Previous studies have shown that expression of Pax6 leads to a clear eye development phenotype at an early embryonic stage (Gao et al., 2020; Jordan et al., 1992; Klann and Seaver, 2019). In a study of the decapod *Exopalaemon carinicauda*, Gao et al. (2020), revealed two Pax6 homologs containing a homeodomain (Hox) domain, that was used as a target for CRISPR.

In the present study, we sought to develop a reliable and effective platform for genomic editing of *M. rosenbergii* in both primary cell cultures and embryos. In aiming to tailor the CRISPR system to prawn cells and embryos, the study included CRISPR delivery methods, editing efficiencies, and editing patterns with various guides.

2. Materials and methods

2.1. Animals and cells

All early developmental stage *M. rosenbergii* embryos used for injection and cell culture were acquired through the BGU breeding program, and a number of egg-carrying gravid females were obtained from Colors Farm Ltd. (Israel). These gravid females were produced in a tank system as follows: A single blue claw male was housed with four to six mature females in a 500-L tank. Each tank was checked daily for the typical male reproductive guarding behavior (Karplus and Barki, 2019) as an indication of gravid females in the tank. Gravid females were then moved to a separate holding aquarium, and the embryos were examined under a light microscope to determine their stage, as described below. One- to four-cell embryos were used for the whole-animal editing platform, while embryos that had already passed the four-cell threshold were kept for 9–13 days up to the eyed-egg embryo stage and then used for the primary cell culture editing platform.

2.2. Embryo stage identification

Embryos were delicately removed from the female with a fine forceps and examined under a light microscope (Nikon H550s, Nikon, Japan). The number of cells was determined by visual inspection. When visual confirmation of cell division was not adequate, cell division was shown by injecting the embryos with Fast Green FCF dye (Allied Chemicals, Thailand), which does not cross membranes, thereby enabling the visualization of cell divisions.

2.3. In-silico identification of Mr-cofilin in the M. rosenbergii transcriptome

The term '*cofilin*' was used as a search keyword in our *M. rosenbergii* embryonic transcriptome library (Abayed et al., 2019). Hits of Pfam analysis were taken for a blastx search until a match to the close crustacean species *Litopenaeus vannamei* (NCBI Reference Sequence: XP_027225677.1) was found. The expression pattern during embryonic development was then generated from the above transcriptome library. The transcript was aligned to the *M. rosenbergii* genome (Levy et al., 2020) to obtain the genomic structure. The genomic structure was then modeled in IBS software (Liu et al., 2015). Finally, the transcript was translated in silico using ExPASy (https://web.expasy.org/translate/) to determine the open reading frames (ORFs).

2.4. Embryo preparation and sterilization

To prevent infection during incubation, fertilized eggs were removed from the brood chamber with fine forceps (or a toothbrush) and placed in a 50-mL tubes, each containing sterile salt water (15 ppt Coral Pro Salt; RedSea, Israel) and 10 μL of methylene blue. Following washing for 10 min in this solution, the eggs were rinsed with sterile salt water containing iodine (0.001 vol%) for 1 min, with sterile salt water containing formaldehyde (4%) for 5 min, and finally with sterile salt water for 5 min. The fertilized eggs were held in a small petri dish of salt water until injected.

2.5. Embryo injections

A ribonucleoprotein (RNP)-Cas9 complex was prepared by mixing 9.5 pmol of synthesized single-guide RNA (sgRNA; IDT, USA) with 5.6 pmol of Cas9 protein (IDT) in a total volume of 1.8 μL. The complex was incubated for 5 min at room temperature before mixing with 0.05% phenol red to a total volume of 4 μL. For Cas9 mRNA delivery, 1 μg/μL GeneArt™ CRISPR Nuclease mRNA (A29378, ThermoFisher) was mixed with similar concentration of gRNA as mentioned above. All injections into *M. rosenbergii* fertilized eggs were performed with IVF micropipettes (Origio, USA), using a pneumatic PicoPump PV830, a vacuum injection system (WPI, USA), and two manual micromanipulators (WPI-M3301R/L, WPI). Pressure was set at 20 psi, and the injection duration set at 100 ms. By using a vacuum pump (Schwarzer Precision, Germany) at a negative pressure of 5 psi, eggs were kept in place for injection with a holding capillary. Then, the injection capillary was inserted into the egg, and successful insertion of the material was verified through the observation of a small phenol red stain at the moment of injection.

2.6. Injection volume calculation

The PV830 injection system included a compressed hydrogen system

to inject the RNP solution. The volume delivered per millisecond was calculated from the equations below using a known injection period of 500 ms followed by the measurement of the diameter of a drop of injected liquid on the tip of the injection capillary. The calculations below show that at an injection rate of 6.72 pL ms^{-1}, 100 ms of injection would deliver 0.67 nL.

$$\frac{Bubble\ volume\left(\frac{4}{3}\pi(r_{bubble\ radius})^3\right)}{t_{Injection\ time}} = Injection\ rate_t\left(\frac{Injection\ volume}{t_{Injection\ time}}\right)$$

$$micron\ cubed\ (\mu m^3) = pico\ Liter(pL)*10^{-3}$$

$$\left(\frac{4}{3}\pi(r)^3\right)*10^{-3}\frac{pL}{\mu m^3} = Injection\ volume\ (pL)$$

$$t\ (milliseconds\ (ms)) = 500ms$$

$$r\ (avg; n=3) = \frac{diameter = 185.8 \pm 2.9\mu m}{2} = 92.9$$

$$\left(\frac{4}{3}\pi(92.9)^3\right)*10^{-3}\frac{pL}{\mu m^3} = 3359.9pL$$

$$Injection\ rate_t = \frac{3359.9pL}{500ms} = 6.72\ \frac{pL}{ms}$$

2.7. Embryo care, DNA extraction, PCR amplification and amplicon sequencing

Injected embryos were transferred to a sterile incubator in small petri dishes, 20–30 embryos per dish, in an aqueous salt solution (15 ppt Coral Pro Salt) and kept at 27 °C for one week. The incubation solution was changed daily, and the eggs were examined visually for dead or malformed embryos. If infection (mainly fungal) was observed, non-contaminated eggs were moved to fresh dishes and further closely monitored. After one week, embryos were separated into individual tubes, and DNA was extracted as follows. Briefly, eggs were submerged in NaOH (0.2 N) and heated to 70 °C for 20 min in a Thermocycler Life Eco (Falc). After rough pipetting to ensure lysis, 50 μL of Tris HCl (0.04 M) were added to neutralize the acidity. DNA was then used as a template for amplification by PCR with specific primers flanking the gRNA. PCR products were cleaned using EPPiC Fast (A&A Biotechnology, Poland) and sent to the Macrogen sequencing lab (Amsterdam, Netherlands) for Sanger sequencing.

2.8. Embryonic cell extraction, editing, and editing monitoring

Prior to the isolation of embryonic cells, *M. rosenbergii* egg-bearing females were disinfected in a methylene blue water bath (5 drops to 10 L water) at least one day prior to cell extraction. Eggs were further disinfected by washing for 10 min in crustacean physiological saline (CPS) (Rotem-Dai et al., 2021) plus antibiotics (PEN/STREP, Biological Industries, Israel) and 0.5 μg/mL of the antifungal preparation Voriconazole (Sigma) in a rotator. Thereafter, the eggs were strained off in a 100-μm strainer (SPL Life Sciences, Republic of Korea) and washed for 1 min in 4% formalin-CPS solution, 1 min in 0.01% iodophor-CPS solution, and finally 10 min in CPS. Eggs were transferred to sterile Eppendorf tubes, containing 200 μL of Halt™ Protease and Phosphatase Inhibitor Cocktail (PI; Thermo-scientific) and 300 μL of CPS and homogenized. The homogenate was filtered through a 100-μm strainer, and the cells that passed through the strainer were collected in a 3-mL petri dish. Thereafter, these cells were transferred to a 15-mL tube and centrifuged at 850*g* for 6 min at 18 °C. The supernatant was discarded, and the pellet was resuspended in 1 mL of PI-CPS and then transferred to a Percoll step gradient comprising 3 mL of 100% physiological Percoll (13.5 mL commercial Percoll with 1.5 mL of CPS × 10), 2 mL of 50% Percoll (physiological Percoll diluted with CPS × 1), 4 mL of 25% Percoll, and 3 mL of 12.5% Percoll. Cells were centrifuged at 850*g* for 30 min at 18 °C. Cell fractions were transferred to a 15-mL tube and washed once with CPS. The cells were seeded at 3×10^6 cells per well in a 6-well plate and grown in Opti-MEM Medium whose osmolality was adjusted to 420 mOsm with CPS. Plates were incubated at 28 °C with 5% CO_2 for 24 h before RNP nucleofection. To monitor editing success, PCR products, using the genomic DNA as template, were sent to the Technion - Israel Institute of Technology (Israel) for next generation sequencing (Miseq Run V2; 2 × 150 bp, assuming 4 M reads per ends per run). The indels caused by the repair of the double-strand breaks through nonhomologous end-joining (NHEJ) were monitored.

2.9. Cell nucleofection

Nucleofection was performed using an Amaxa P3 Primary Cell 16-well Nucleocuvette Strips kit (V4XP-3032; Lonza, Switzerland) and an Amaxa 4D-Nucleofecter (Lonza). The RNP Cas9 complex was formed by mixing 2.64 μL (163 pmol) of Cas9 62 μM (1,081,059; IDT) with 1.76 μL (176 pmol) of sgRNA 100 μM (IDT) in P3 nucleofection buffer (total volume of 11 μL); the mixture was incubated at room temperature for 20 min. For mRNA Cas9 delivery, GeneArt™ CRISPR Nuclease mRNA (A29378; ThermoFisher) was used in a final concentration of 0.06 μg/μL. An amount of 4×10^5 primary cells were harvested, washed once in Opti-MEM, and resuspended in 28.6 μL of P3 nucleofection buffer. The cell suspension was mixed with RNP-Cas9, and 20 μL of the cell-RNP suspension was transferred to each of two wells of the 16-well strip nucleocuvette. Cells were electroporated using program CL-137 on the 4D-Nucleofector. Immediately after nucleofection, 80 μL of Opti-MEM + 10% FBS was added to each well at room temperature, and all 100 μL of cell suspension were transferred to a 96-well plate containing 50 μL of pre-warmed medium. The plate was incubated at 28 °C under 5% CO_2. Edited cells were harvested three days after nucleofection. For DNA extraction, cells were suspended in culture medium and centrifuged at 11,000*g* for 5 min. The supernatant was discarded, and the cells were resuspended in 10 μL of NaOH (0.2 N). Tubes were heated to 70 °C for 20 min and vortexed before the addition of 50 μL of Tris HCl (0.04 M).

2.10. Phenotypic proof of concept

M. rosenbergii embryos start developing eyes approximately one week after fertilization, and therefore eye development was used in the present study as an early indicator of successful genomic KO. Zygote to second nuclear division embryos at 3–7 h post fertilization (HPF; Ling (1969b)) were taken from a gravid female and sterilized as described above. Three different guides were injected, *Hox3* ($n = 44$) and *Hox4* ($n = 41$), aimed at the *Pax6* Hox motif as a means of maximizing KO effectiveness, and *Mr-cofilin* ($n = 28$) as a positive control for the editing. Non-injected embryos served as the negative control for the phenotype. Individual gRNA and primers are detailed in Table 1. After injections of 0.67 nL (for each embryo), the embryos were kept at 28 °C for 20 days up to hatching, with monitoring every two days as described above. Two hatchlings from each treatment were taken for Sanger sequencing, and the remaining hatchlings ($n = 3$ for each group) were examined under a microscope (Nikon H550s, Nikon, Japan) for phenotypic outcomes in

Table 1
Guide RNAs and primers for Sanger sequencing.

Sequence	5′ to 3′ sequence
Hox3 gRNA	TCTTTGCAGCCAGTCTCTCG
Hox4 gRNA	TCTCGCGGGCAAATACGTCA
Hox3,4 forward primer	TTTCACTGTAATGATTTTTCAAGAGC
Hox3,4 reverse primer	CAGACAAATAACCTTCTAAGCAAGGG
Mr-cofilin gRNA	CATATGACTAGCTGGCCACA
Mr-cofilin forward primer	TATGGCCGAAGCATCTTATGAATGT
Mr-cofilin reverse primer	CACAACTCTTTCCACACACCAACAA

the developing eye. Eye area was calculated by measuring the length and width of the eye in perpendicular lines, then multiplying the measurements and halving the result ($Eye\ area = \frac{Eye\ length * Eye\ width}{2}$).

2.11. Sequencing and statistical analyses

Sequences from Sanger sequencing were analyzed by the Synthego ICE program (https://ice.synthego.com/#/) and charted according to

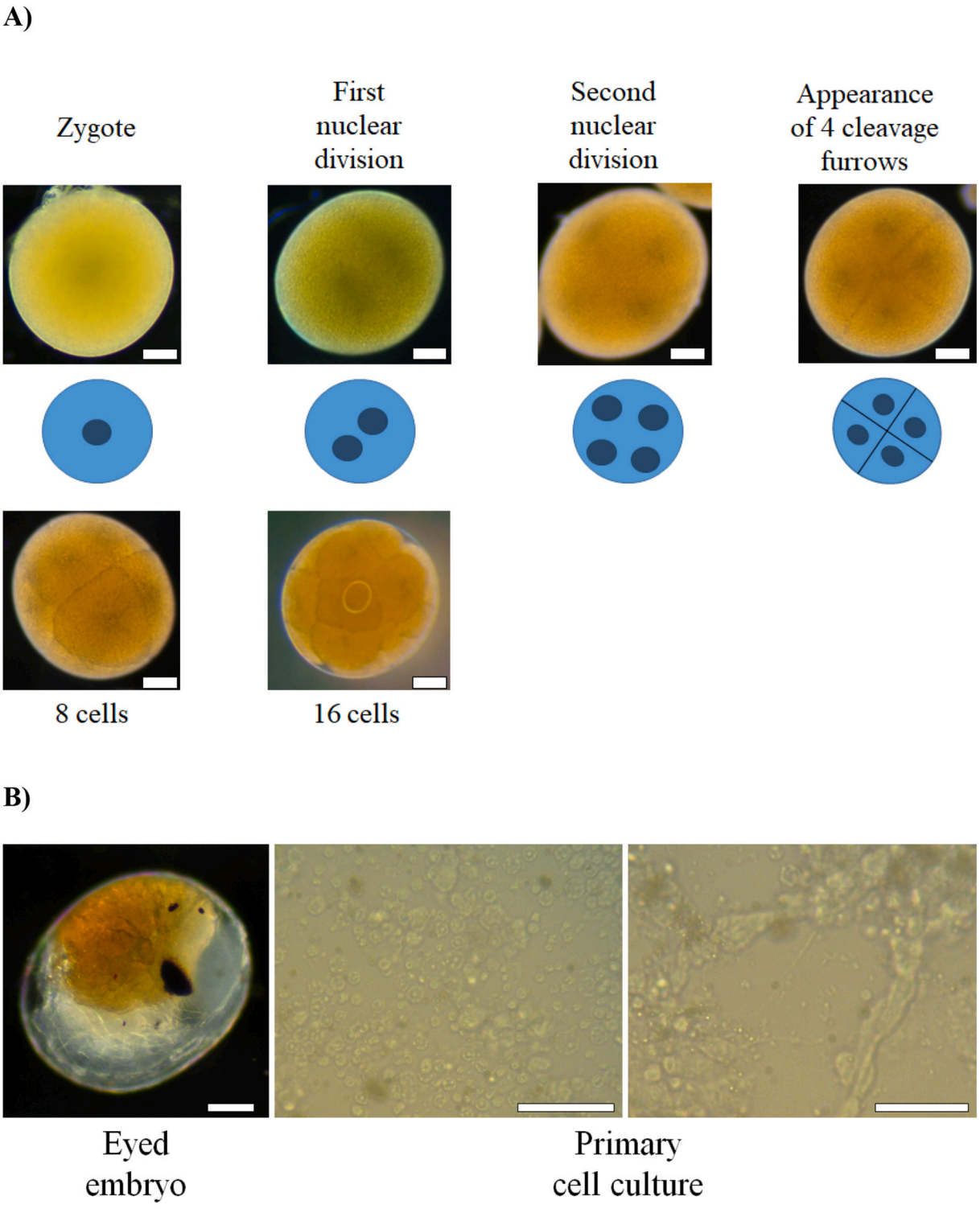

Fig. 1. Early embryonic development of *M. rosenbergii.* A) Early nuclear and cell divisions of *M. rosenbergii* embryos. The dark areas in the eggs are the nuclei, as shown in the schematic representation (in blue) below the photographs. Two initial divisions of the nucleus occur prior to cell formation at 4 and 6 h post fertilization (HPF). At 8 HPF, the egg divides into 4 cells (rather than splitting into two), and one hour later divides again into 16 cells. Subsequent divisions occur at 1.5-h intervals. Scale bars are 100 μm. B) Eyed eggs and cells in culture from eyed embryos. Left - Eyed embryo: Eye development starts at 9–10 days post fertilization, and these embryos contain a large number of cells that are suitable for extraction. Middle and right - Primary cell cultures of extracted cells containing various types of cells. All scale bars are 100 μm. (For interpretation of the references to colour in this figure legend, the reader is referred to the web version of this article.)

the KO score. Crispresso2 (https://crispresso.pinellolab.partners.org/submission (Clement et al., 2019) was used to determine the editing efficiency of various guides in the genomic editing experiments using the default settings of the website. Comparisons and statistical analyses were performed with Statistica v13.3 software (StatSoft, Ltd., USA), using one-way ANOVA, followed by a post hoc Tukey's HSD test with $p \leq 0.05$ regarded as a significant difference. All percentage data was converted to decimal form and transformed by applying the square-root of the tangent. To test the difference in the pattern of editing between injected embryos and cells in primary culture across a 40-bp window, two analyses were used: First, a non-parametric two-sample Kolmogorov–Smirnov test and a permutations test on the absolute difference in skewness between the two editing distribution patterns were used. Second, data from embryos and cells were pooled and then sampled without replacement to generate two random sample distributions. The absolute difference (two-sided test) in skewness between the two random sample distributions was calculated. This procedure was repeated 10,000 times. Permutation *P* values were calculated as the proportion of cases in which the absolute difference obtained during the random simulations was equal to or greater than that detected in the original data set. These analyses were performed using MATLAB version 2020a (The MathWorks, Inc., 2020, USA).

3. Results

To tailor the genome editing method in *M. rosenbergii*, we studied two time periods during embryonic development, namely, the period of early divisions of the embryonic cells that were used to construct the edited embryos and the eyed-embryo stage, 10–16 days after fertilization. Immediately after fertilization, upon visual inspection, the eggs appear bright yellow and entirely filled with yolk vesicles, while under a light microscope, a darker mass (the nucleus) can be seen at the center of the cell. At 3–4 HPF, the nucleus splits into two (first nuclear division), but no cell wall is visible (Fig. 1A, top). At 6 HPF, the two nuclei divide again, and only at 8 HPF are the first cellular divisions into four cells, each with a nucleus at the center, visible. The next two cell divisions are correlated with nuclear divisions, 9 HPF for the 8-cell stage, and 10.5 HPF for the 16-cell stage (Fig. 1A, bottom). When the eyes started to develop and became visible as black slits on the sides of the embryo (eyed-embryo stage, Fig. 1B, left), cells were extracted from the embryos and cultured for 24 h prior to electroporation and editing manipulations (Fig. 1B, middle and right). At this stage, a considerable quantity of cells could be extracted to establish a primary cell culture (Fig. 1B, right).

A key word search for "*cofilin*" in our *M. rosenbergii* embryonic library (Abayed et al., 2019) revealed a transcript of 1061 nucleotides. This transcript was named *Mr-cofilin* and was submitted to GenBank® (accession number OL743530). A BLAST search of this transcript in the NCBI gave the highest similarity to a transcript of *Macrobrachium nipponense* (Sequence ID: CP062035.1), with an E value of zero and 98.68% identity. This transcript was highly expressed in all embryonic stages that are represented in the *M. rosenbergii* embryonic library (days 1, 3, 5, 11 and 17; see Fig. 2A). A BLAST search in the genome of *M. rosenbergii* (Levy et al., 2020) revealed that the genomic sequence of *Mr-cofilin* contains 5 exons, as shown in Fig. 2B. The sgRNA design for the *Mr-cofilin* gene was identified by the IDT online tool.

In our *M. rosenbergii* embryonic library (Abayed et al., 2019), *Mr-cofilin* showed high relative expression throughout embryonic development (Fig. 2A), with day 1 showing a read count average ± standard error of 14,604 ± 3779 and day 3, a slight drop to 9076 ± 601. The read counts for days 5, 11, and 17 were 12,682 ± 1210, 14,358 ± 479, and 13,531 ± 770, respectively. As may be seen in Fig. 2B, the genomic structure of *Mr-cofilin* is comprised of five exons and four introns, with two long introns over 4000 bp and two short introns under 150 bp. The mature mRNA comprises 1406 bp with an ORF of 447 bp and long 5′ and 3' UTRs. The guide RNA selected for the present study is situated at the 3' UTR at position 769 (Fig. 2C).

Mr-cofilin was found to be a highly expressed gene (Fig. 2A) whose editing did not cause fatalities; it was therefore used for the study of the optimal delivery method of Cas9 into the prawns. Our ICE results for experiments conducted in line with recommendations from the literature for the use of either Cas9 mRNA plus the guide or RNP (Gui et al., 2016; Kumagai et al., 2017) showed that in *M. rosenbergii* mRNA injection into embryos was not as effective as RNP (Fig. 3), with an average of 24.7 ± 14.8% successful editing for mRNA ($n = 5$) versus 73.4 ± 18.2% for RNP ($n = 6$). The same trend was evident for the primary cell culture, with no detectable editing for mRNA versus 42 ± 1% successful editing for RNP ($n = 8$ for both).

To determine the optimal schedule in terms of cell division for successful embryonic editing, embryos of different cell numbers, from fertilization up to the 32-cell stage, were injected with Cas9 RNPs (Fig. 4A). ICE results for the first two stages of no cellular divisions (1 cell) and the first division (4 cells) were similar, averaging 43.8 ± 14.2% (n = 5) and 41.6 ± 8.3% (n = 6), respectively. Only at the 8-cell stage was there a significant drop in editing success ($p = 0.02$), with 11 ± 7.2% (n = 6) editing efficiency. The 16-cell stage appeared to be unaffected, with only a single case showing 5% editing efficiency, and the rest showed no editing (n = 6). The same trend was evident for the 32-cell stage, with an average of 2.3 ± 2.3% editing efficiency. These results enabled us to narrow the effective injection period to embryos of one to four cells. Experimentation aimed to adjust the injection volume of Cas9 RNPs for 1-cell to 4-cell embryos yielded the following ICE results for six different volumes (doubling the volume in each step; Fig. 4B): 84 pL gave 15.2 ± 16.6 editing efficiency; 168 pL, 27.6 ± 17.3%; 335 pL, 28.7 ± 7.1%; and 670 pL 43.2 ± 17.7%; a further increase in volume to 1.34 μL did not result in an increase in effectiveness, giving 30.3 ± 12.4%. No significant difference was seen in embryo survival between the volumes checked.

Based on the above calibration results, 80 gRNAs targeting 23 different genes were tested. Percentage editing efficiency was calculated and showed that guide effectiveness varied in both edited embryos and embryonic cells in culture (Fig. 5). The rate of success in injected embryos ranged from no editing (0%) to 100% editing efficiency ($n = 40$). In contrast, primary cell culture showed a narrower range, with editing efficiency ranging from 0% to a maximum of 64.3% ($n = 69$). *Mr-cofilin* independent repeats were constant, averaging at 95.4 ± 2.7% ($n = 3$) for injected embryos versus 38.7 ± 3.4% ($n = 7$) for primary cell culture.

Crispresso 2 visual representation (Clement et al., 2019) showed a striking difference between the editing patterns of the embryo and the embryonic cells in culture. To depict this phenomenon graphically, Fig. 6A shows three representative independent *Mr-cofilin* injections into embryos resulting in similar deletion patterns, with most deletions missing the first base upstream of the cut site and gradually decreasing further away to each side of the cut site. In contrast, embryonic cells in primary cell culture (Fig. 6B) showed a different editing pattern, with most deletions being in the same base, one upstream of the cut site with a positively skewed pattern towards the 3′ end of the gRNA showing a gradual drop to 0. These differences in patterns between embryos and cells were consistent with the patterns obtained using other guides targeting other genes (e.g., supplementary Fig. S1). The above difference in the pattern of editing between embryos and cells was found to be statistically significant using the non-parametric two-sample Kolmogorov–Smirnov test ($p < 0.0001$) and a permutations test on the absolute difference in skewness between the two patterns across a 40-bp window ($p < 0.001$).

Phenotypic proof of concept was provided by investigating the effects of KO on eye development in embryos, which later hatched into larvae. Initial comparisons of eye size at 15 days post injection (Fig. 7A) showed a significant difference ($p < 0.001$) between *Hox3,4*-injected embryos on the one hand and *Mr-cofilin*-injected and non-injected embryos on the other. Average eye size was 2126 ± 164 mm^2 for *Hox4*-injected embryos (n = 6) and 2789 ± 183 mm^2 for *Hox3*-injected embryos (n = 6); significantly higher values were obtained for *Mr-cofilin*-

A)

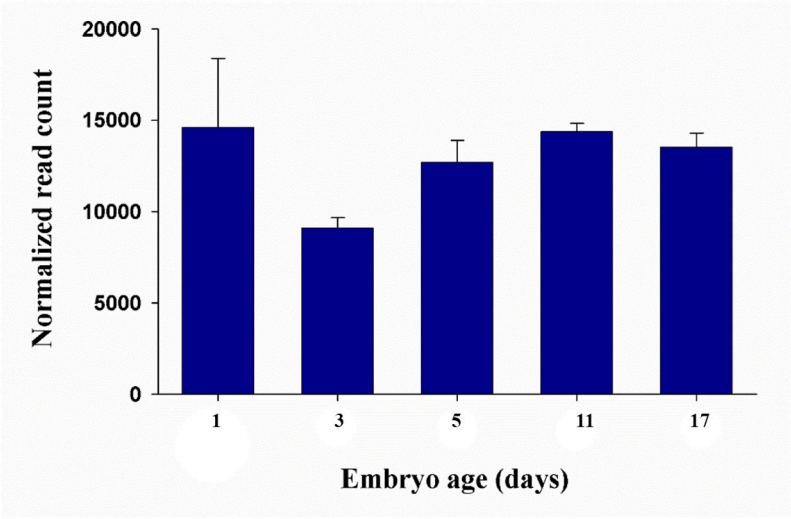

B)

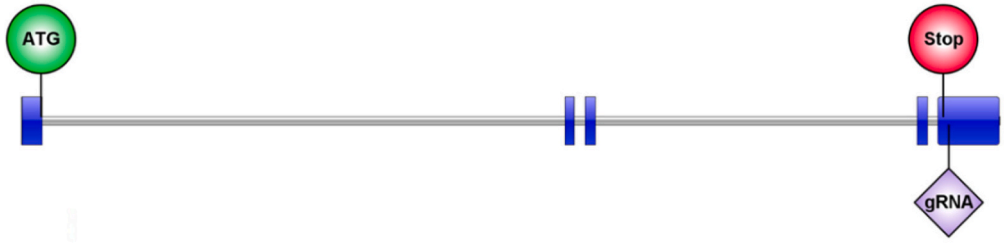

C)

```
   1 cgatgacatttcagcggctgtaagcactgttcccattggccgaaagtctgcattgtggggccgagagagaggcgacgggccaat  84
  85 gggcggcggcgtgacaaaagctctcgtcaccggacggactcggcggagtgatatatgacgtcactactcgcactacgccccttc 168
 169 aagttgaacatcctcatcggagtcagtcactaatagtcagtctgtgttccctagtgatcagaactttggtgaattggatttacg 252
 253 atggcttcaggagtccaagtatcggatacagtaatagagtacttccaacaaataaagaagggaaagatgtataggtacataatc 336
   1  M  A  S  G  V  Q  V  S  D  T  V  I  E  Y  F  Q  Q  I  K  K  G  K  M  Y  R  Y  I  I  28

 337 ttccacattaaagatgacaaggtcattgatgttgaaacgactggagatagagacgctagttatgatgactacttaaactacctg 420
  29  F  H  I  K  D  D  K  V  I  D  V  E  T  T  G  D  R  D  A  S  Y  D  D  Y  L  N  Y  L  56

 421 gtaaatttggggcctgaacagtgccgttatggcatctatgattttgaatacgatcatcagtgccagggaacgacagattctacg 504
  57  V  N  L  G  P  E  Q  C  R  Y  G  I  Y  D  F  E  Y  D  H  Q  C  Q  G  T  T  D  S  T  84

 505 aggaagcagaaacttttcctgatgtcttggtgcccagatactgccaagatcaaaaagaagatgctgtattcatcaagctttgat 588
  85  R  K  Q  K  L  F  L  M  S  W  C  P  D  T  A  K  I  K  K  K  M  L  Y  S  S  S  F  D  112

 589 gcccttaaacaatcattggaaggcataggaaagtacatacaggctacagatatggccgaagcatcttatgaatgtgttttggac 672
 113  A  L  K  Q  S  L  E  G  I  G  K  Y  I  Q  A  T  D  M  A  E  A  S  Y  E  C  V  L  D  140

 673 aagatgcgctctactgacagaacctaagttagtgatgggaggcccctctgttctggagagcccccgctgtatttgaggggtccc 756
 141  K  M  R  S  T  D  R  T  *                                                          148

 757 tttgtctctaccgccctgtggccagctagtcatatgtgggccacaatcatgctatccacgcagcatgaagagaactttgtttaa 840
 841 ttatttttattcacaatttgttggtgtgtggaaagagttgtggggaaacagtgtttcaccagaagaaaggttaggcttgatac 924
 925 aaatgccatgtgggagagtggaccggctttaaagttaggacaaatagtcttgacattaaagctggtcccaagtgatgtgggaga 1008
1009 ggcagtgtttcatgcattgctacagagttggcagaggagagttagtattaaatataaatgctcttccatacgtattttgtccca 1092
1093 ttgtatgtgatcttggatctttcacatcttcatagatataataagctttatataaacagtatagccatttaccatttattggct 1176
1177 ccaaaaattattttattaactgctcaaaatccttaattgcatcagcttcattatgtgaatcatgaatttagtttaaaaagggat 1260
1261 ttttttatgatttaaatgtaggatcaacttgtcagaataaatttctttttaatgttggtgattttatttcatcttgcctttggt 1344
1345 taaagaaactgcagttgaaaatcgtcaactggatgtgattatgatcatggatattaagtttt                        1406
```

Fig. 2. *Mr-cofilin* expression pattern, genomic and transcript structure in *M. rosenbergii.* A) *Mr-cofilin* expression pattern during embryogenesis constantly shows high expression in both sexes. Bars represent means and standard errors of normalized read counts. For day 1, $n = 5$ three biological repeats from male embryos and two from female embryos, and for all subsequent days $n = 6$, three repeats of each sex. B) The genomic structure of *Mr-cofilin* is comprised of five exons (blue squares) and four introns (gray lines), totaling 12,302 bp. C) Mature mRNA comprises 1406 bp with an ORF of 477 bp and long 5′ and 3' UTRs; the guide RNA is situated at the 3' UTR 769 bp. The putative translated protein is 148 amino acids long and contains actin de-polymerization factor (ADF)/cofilin-like domains. Start and stop codons are highlighted in green. (For interpretation of the references to colour in this figure legend, the reader is referred to the web version of this article.)

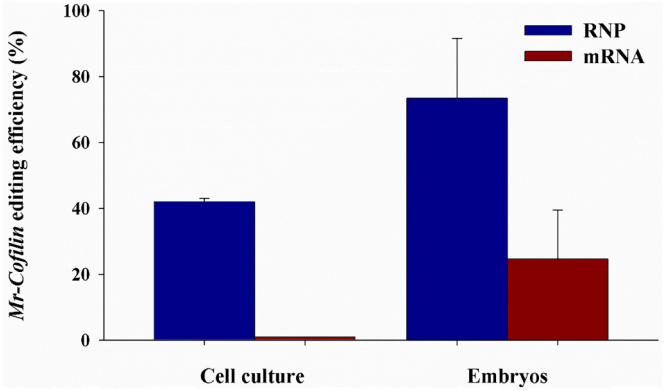

Fig. 3. Comparison of Cas9 mRNA versus ribonucleoprotein (RNP) in embryos or embryonic cells in primary cell culture for *Mr-cofilin* editing. Injections into 1-cell to 4-cell embryos and nucleofections to primary cell culture with either Cas9 mRNA (in red) or RNP (in blue) with *Mr-cofilin* gRNA. For embryos, RNP editing efficiency averaged 73.4 ± 18.2% (n = 6), and mRNA editing efficiency, 24.7 ± 14.8% (n = 5). For cell culture, only in RNP editing was successful at 42 ± 1% (n = 8). Bars represent means of editing efficiency according to ICE results ± standard error. (For interpretation of the references to colour in this figure legend, the reader is referred to the web version of this article.)

injected and wild-type embryos, namely, 4382 ± 321 mm^2 (n = 5) and 3647 ± 167 mm^2 (n = 5), respectively (Fig. 7B). Survival rates of the injected embryos averaged 15%, with 7 of 44 and 5 of 41 hatching into larvae in *Hox3*- and *Hox4*-injected embryos, respectively. Hatched larvae with *Pax6* KO exhibited smaller eyes than the controls, together with a deformity of the crystalline cones (Fig. 7C). Sanger sequencing confirmed that the *Pax6* KO affected 100% of the cells (Fig. 7D).

4. Discussion

Here we present the first genomic editing system in the prawn *M. rosenbergii*, calibrated for maximum editing efficiency for embryos (Fig. 8 Top) and embryonic primary cell cultures (Fig. 8 Bottom), with the two platforms providing different rates of editing efficiency using Cas9 RNP with various gRNAs (Fig. 8 Right). The most notable distinction between the two platforms was the relatively high editing efficiency in embryos versus much lower rates in embryonic cells in primary culture. These differences can be explained by the different methods of Cas delivery, namely, direct injection into whole embryos at the 1-cell to 4-cell stages versus the less specific electroporation in primary cell culture, which results in a reduction in editing efficiency (Lino et al., 2018). Moreover, the injections into embryos were calibrated for the optimal volume and for the optimal time as close to fertilization as possible, since the Cas protein needs to reach only one to four genomic sites, and DNA replication will carry the mutation from the first few edited cells to the entire embryo (Hwang et al., 2013). In contrast, during electroporation, the primary cell culture system contains about 200,000 cells at various stages of the cell cycle, and thus the resulting delivery into the cells in the primary culture system might be more variable in terms of successful editing. Additionally, the doubling time of the above primary cell culture is 9 days (Weil personal communication), so the masking effect of unedited replicating cells after electroporation in negligible (the experiments lasted only 4 days from cell extraction to sequencing).

During the calibration process, we showed that RNP yielded higher editing rates than *Cas9* mRNA in both platforms. mRNA yielded only 24.7% of edited embryos and no detectable edits in cell culture, in contrast to other crustacean species showing high rates with mRNA administered by microinjection and even in cell cultures (Xu et al., 2020). The sequence of the gRNA also has a major influence on editing efficiency, with effectiveness ranging from 0 to 100% in embryos and 0–64% in cells, as has been previously shown in plants and arthropods, with multiple guides yielding different efficiency outcomes (Hu et al., 2019) (Lino et al., 2018) based on the different genes and gRNA location in the genomic sequence.

Finally, based on the above parameters and the calibration of the CRISPR system in *M. rosenbergii*, a phenotypic proof of concept was provided by targeting *Pax6* to produce an early eye phenotype change (Gao et al., 2020). It is noteworthy that the above phenotype change was manifested despite the fact that significant cases of editing included three base frame shifts that could still yield an active protein. Such a frame shift might not temper the activity of the mature protein but might introduce exon skipping instead (Tuladhar et al., 2019).

DNA repair systems – a highly studied aspect of cell function – are a crucial part of the CRISPR/Cas9 editing methodology. The repair of the

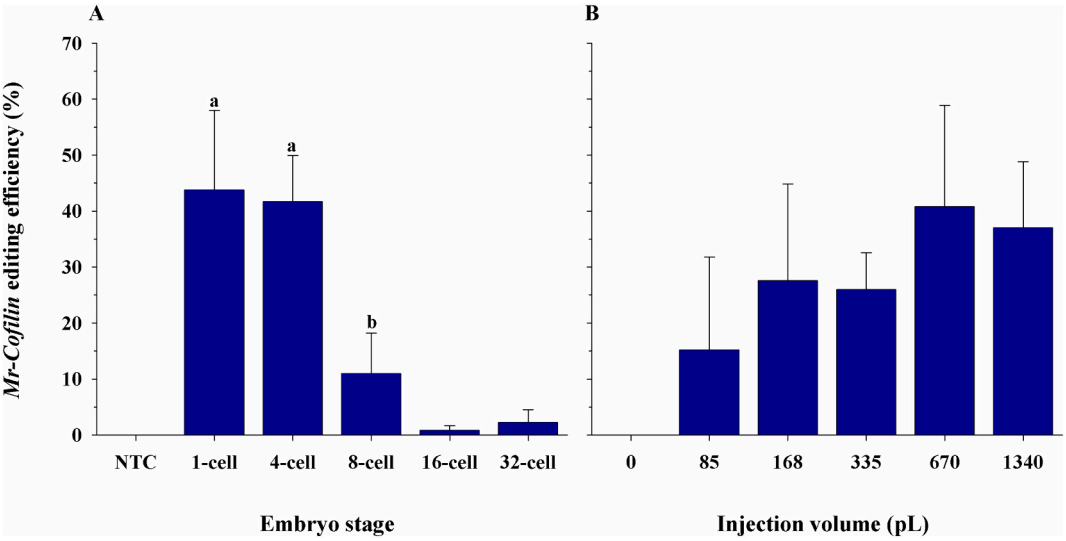

Fig. 4. Calibration and efficiency of RNP injection into *M. rosenbergii* embryos. A) RNP injections at different early stages of *M. rosenbergii* embryo cell divisions. Injections of Cas9 RNP, with *Mr-cofilin* gRNA, were administered to embryos from fertilization (1-cell) until the 32-cell stage. Number of cells refers to cell divisions; n = 6 for all stages. Bars represent means of editing effect according to ICE analysis of Sanger sequencing ± standard error with 'a' and 'b' signifying a significant difference between the groups (one way ANOVA, p = 0.02). B) Calibration of Cas9 RNP conjugated with *Mr-cofilin* gRNA injection volume into *M. rosenbergii* 1-cell to 4-cell embryos. Bars represent ICE analysis of Sanger sequencing deletions (percentage), means ± standard error. For all volumes n = 6.

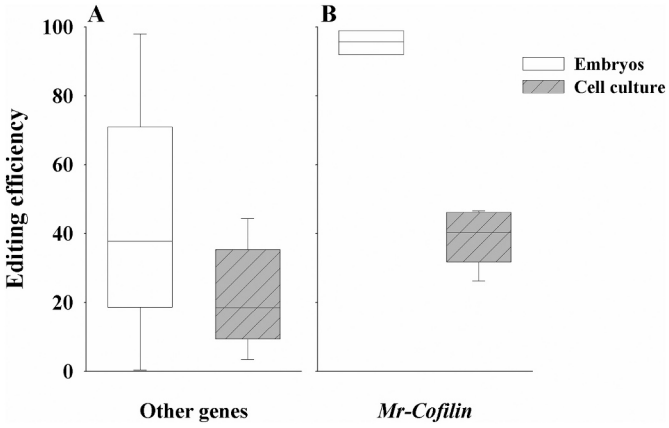

Fig. 5. Editing efficiencies under optimal conditions using gRNAs from various genes in embryos and primary cultured *M. rosenbergii* embryonic cells. Results of next generation sequencing showing editing efficiencies of various targets, including A) 23 different genes and 80 guides for 40 samples in embryos (white) and 69 in primary cell culture (gray), and B) 3 *Mr-cofilin* repeats in embryos (white), and 7 *Mr-cofilin* repeats in in primary cell culture (gray). The results are given for 1-cell to 4-cell embryos injected with 670 pL of RNP solution and cell nucleofection of several different broods.

double strand break through NHEJ was evident in the pattern of deletions occurring around the Cas9 cut site. The NHEJ repair machinery removes, adds, or modifies a few bases to each side of the break before repair, usually resulting in a small deletion on both sides of the break (Davis and Chen, 2013). A striking phenomenon revealed in the present study was a radically different repair pattern for *M. rosenbergii* embryos versus primary cell cultures. In embryos, we obtained a typical pattern of a few deletions on both sides of the cut site, similar to other embryo KO experiments in other crustaceans (Gui et al., 2016; Kumagai et al., 2017; Martin et al., 2016). In contrast, in the primary cell culture, the deletions were positively skewed to the 3′ end of the guide, away from the protospacer adjacent motif (PAM). It is posited that these differences could be due to the environments of the cells in their native embryonic tissue versus that of the single-layered primary culture, causing Cas9 to stay firmly attached to the PAM (Sternberg et al., 2014) This 'attachment' might prevent the access to the upstream strand of repair proteins, such as 5′ exonucleases, resulting in the prevention of the ablation of the strand and hence in the observed 3′ skewness of the repair in the cell culture. Contrary to the above, in the embryos, Cas9 detaches normally, and the repair machinery has access to both strands, leading to a normal distribution of deletions around the cut site. Another hypothesis that could explain this phenomenon suggests different machineries for the repair mechanism in the two cases, possibly caused by the difference in the cell types, i.e., initial stem cells in the newly formed embryo vs. mostly differentiated cells on the primary cell culture (Ceccaldi et al., 2016; Wilson et al., 2018). These differences in the repair patterns between the two platforms should be studied further both for basic scientific understanding and for their applied merit.

Further development of genome editing in aquaculture will require regulatory attention. This is emphasized by the fact that genetically engineered food items, such as fruits and vegetables (Jaganathan et al., 2018; Turnbull et al., 2021) and in recent years even fish (Edvardsen et al., 2014; Kishimoto et al., 2018), have already been developed but

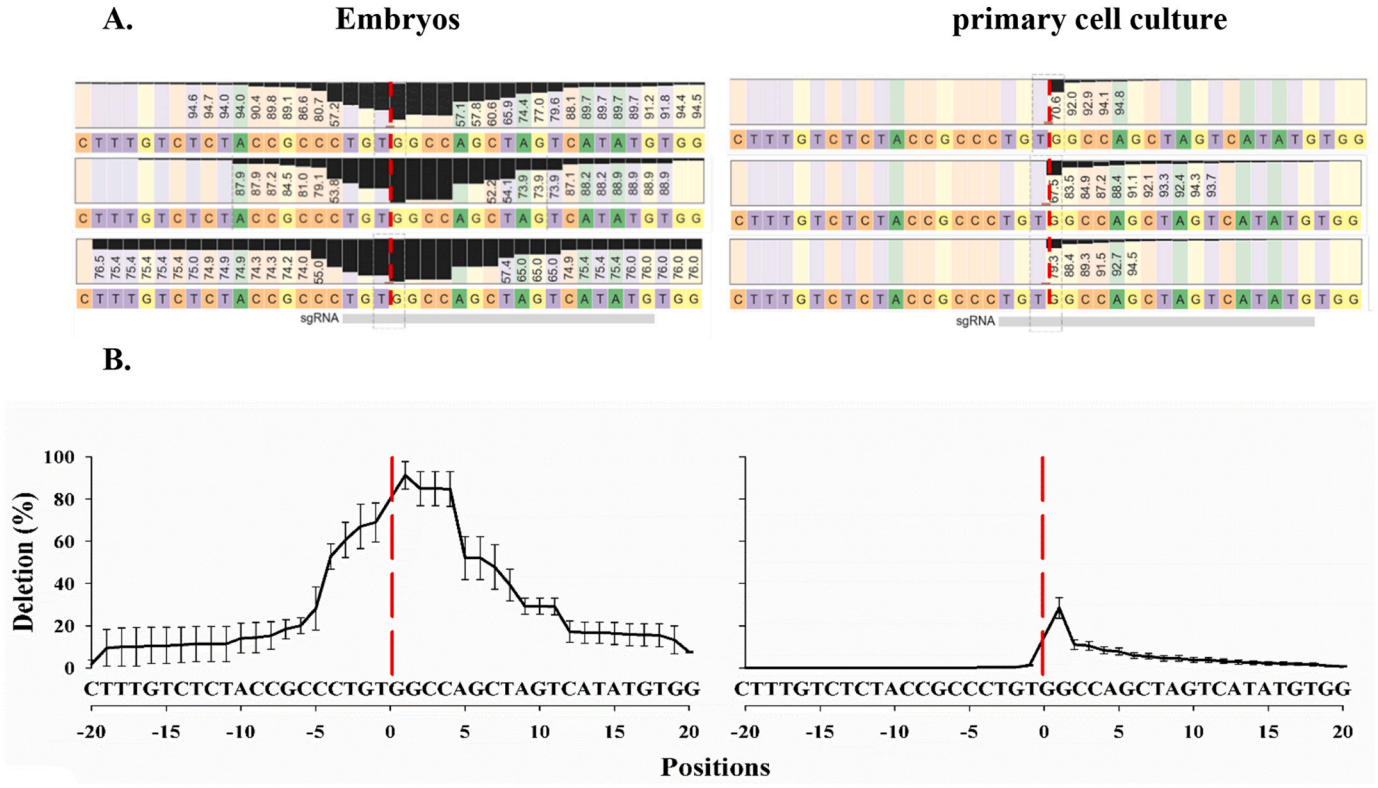

Fig. 6. Editing patterns in *M. rosenbergii* embryos versus embryonic primary cell culture. A) Crispresso2 representation of editing pattern in *M. rosenbergii* embryos and primary cell culture with *Mr-cofilin* sgRNA. *Mr-cofilin* sequence is presented at the bottom of each block with indication of guide location at the bottom (gray line). Red dotted line signifies the cut site, and black bars represent deletions (percentage) at each position. Numbers represent unedited cases (percentage) at a given position. B) Graphic representation of the distribution of averaged deletions per position in embryos (left) and cell culture (right), $n = 3$ for both, with significant differences ($p < 0.001$) between the two distribution patterns using a permutations test. Red dotted lines signify cut sites, bars represent standard error. All values upstream of the cut site in primary cell culture were 0%. (For interpretation of the references to colour in this figure legend, the reader is referred to the web version of this article.)

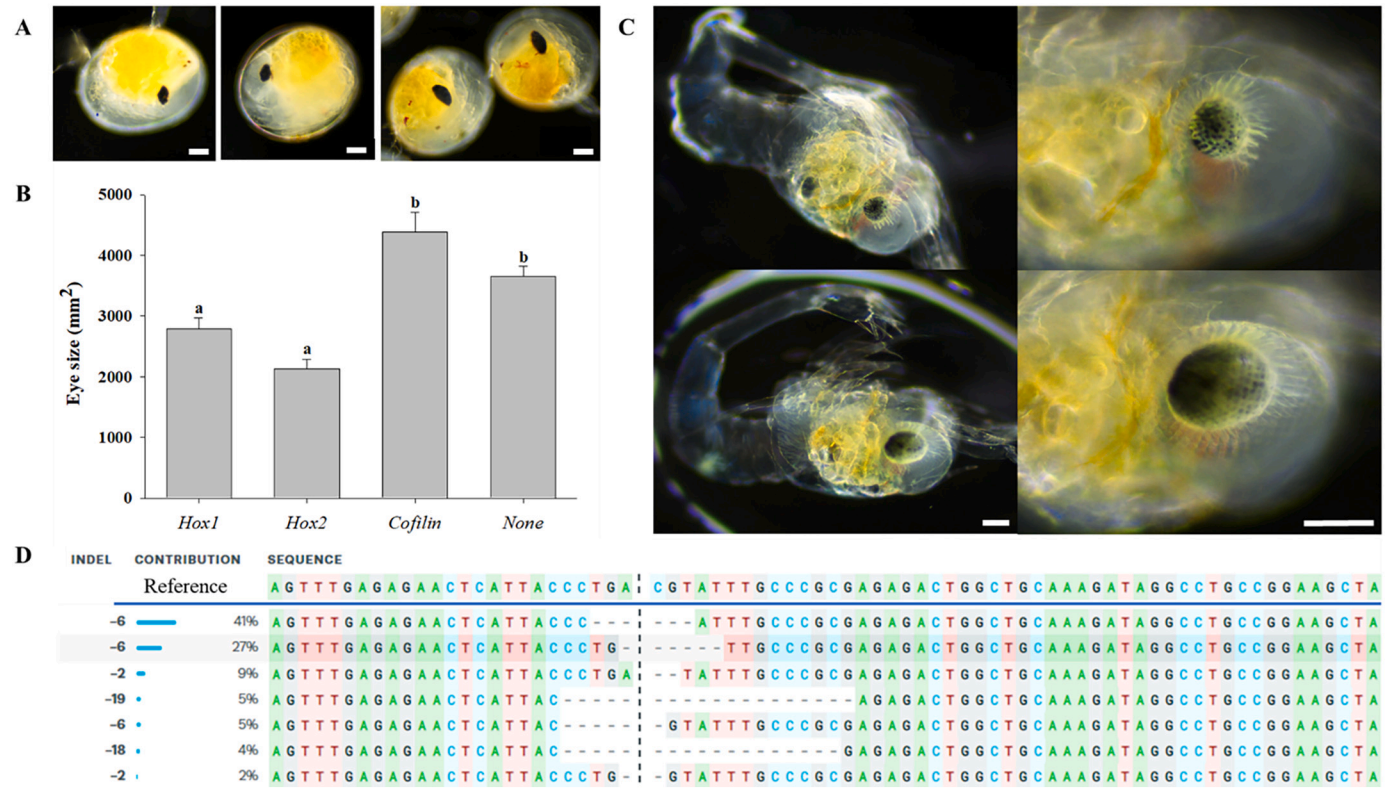

Fig. 7. Phenotypic proof of concept of editing through eye development in *M. rosenbergii* embryos and larvae. A) Representative images of 15-day-old *M. rosenbergii* embryos injected with different gRNAs: left - *Hox4*, middle - *Hox3* and right - wild type. B) Eye area (mm^2) of 15-day old embryos for each gRNA; bars represent means ± standard errors of eye area and 'a' and 'b' represent significant differences between the groups. C) Representative pictures of stage-1 larvae: top – *Hox4*-injected larva and bottom – wild-type larva. D) ICE analysis of Sanger sequencing results of samples for the *Hox* domain of *MrPax6*: top – reference sequence; bottom – *Hox4*-injected larva Sanger sequencing. 'Indel' indicates number of deleted bases found in each sequence, 'Contribution' indicates the percentage of amplicons with similar sequences, and 'Sequence' indicates a window around the cut site. All scale bars are 100 μm; gRNA sequences are presented in Table 1.

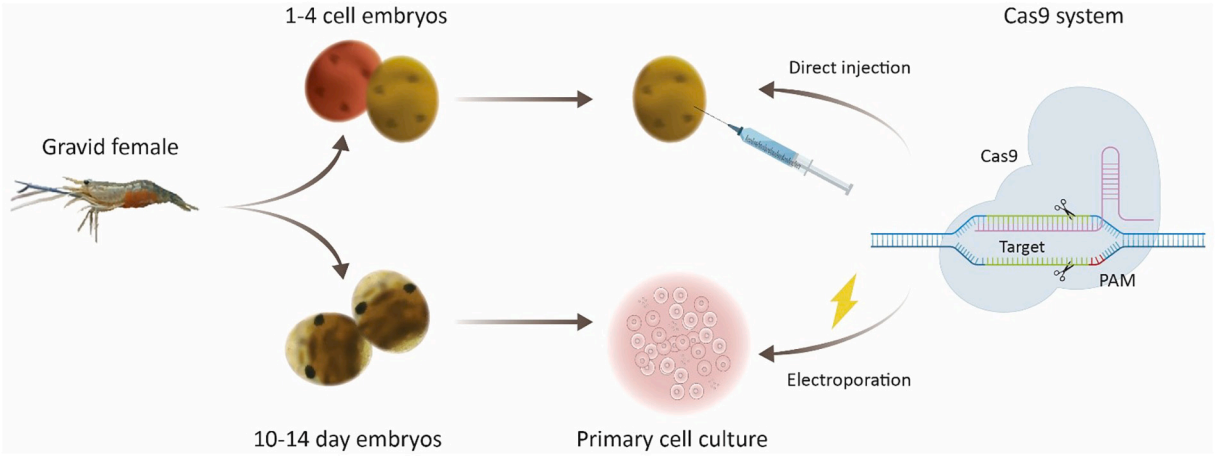

Fig. 8. Schematic representation of editing platforms in *M. rosenbergii*. Gravid females are collected after fertilization (left). One to four-cell embryos were taken for direct Cas9 RNPs injection (top). Ten to twelve–day old eyed-embryos were used for cell extraction followed by primary cell culture (bottom) and subjected to electroporation in the presence of Cas9 RNPs. The RNP Cas9 system (right) penetrates the cell in both platforms and cleaves the DNA according to the gRNA sequence causing a double strand brake.

regulatory guidelines have not kept pace with these developments. In crustaceans, while successful editing in some studies has led to the production of modified adult animals (Gui et al., 2016; Kumagai et al., 2017; Martin et al., 2016), no product known to us uses genetically modified animals, and thus regulatory attention has not yet devoted to this branch of aquaculture. As the technology becomes more widespread and enters public consciousness (Scheufele et al., 2021), further studies should be devoted to the prevention of off-target editing and to accurate assessment of the changes made by the CRISPR/Cas9 system.

In conclusion, in the present study we established two platforms of CRISPR systems, one in cells and the other in an entire organism. The use of edited cells in culture, other than being a higher throughput research tool, could in itself contribute to the establishment of cell lines that could serve as a starting material for artificial seafood products, as has

been seen with bovine muscle (Furuhashi et al., 2021) and fish (Rubio et al., 2019). The present study also forms the basis for future work aiming at safely creating selectively bred lines of *M. rosenbergii* with unique traits and benefits for both aquaculture and biocontrol through minor and precise editing.

Author contribution

This study was conceived and designed by JM AS and ED.A. JM, MS, RM, HW and DF collected the gravid females for the study. JM, MS, RM HW and EH Designed the guides and primers for this study. JM, MS, DP, HW and TL injected embryos. Primary cell extraction for culture was Preformed by JM, RM, MS, DP, SW, HW and EH. JM, RM, MS, DP, SW, HW and EH preformed electrophoresis on cell culture. JM, RM, MS, RO, DF, HW, EH and AH reviewed and analyzed the sequencing data. JM, RM and MS performed the in silico analyses. JM and RM performed bioinformatics analyses. All authors analyzed and interpreted the data. The manuscript was written by JM and AS and reviewed and approved by all co-authors.

Declaration of Competing Interest

The authors declare that they have no known competing financial interests or personal relationships that could have appeared to influence the work reported in this paper.

Acknowledgements

Prawns were supplied by the Tiran group, through Colors Farm Ltd., and by Enzootic Ltd. The study was partially funded by the CRISPR-IL consortium of the Israel Innovation Authority and a grant from the Ministry of Science & Technology, under The Taiwan-Israel Collaboration program (grant no 001994). We wish to thank Prof. Ofer Ovadia for his suggestions and comments regarding the statistical analyses.

Appendix A. Supplementary data

Supplementary data to this article can be found online at https://doi.org/10.1016/j.aquaculture.2022.738391.

References

Abayed, F.A.A., Manor, R., Aflalo, E.D., Sagi, A., 2019. Screening for Dmrt genes from embryo to mature *Macrobrachium rosenbergii* prawns. Gen. Comp. Endocrinol. 282, 113205.

Bamburg, J.R., 1999. Proteins of the *ADF/cofilin* family: essential regulators of actin dynamics. Annu. Rev. Cell Dev. Biol. 15, 185–230.

Ceasar, S.A., Rajan, V., Prykhozhij, S.V., Berman, J.N., Ignacimuthu, S., 2016. Insert, remove or replace: a highly advanced genome editing system using CRISPR/Cas9. Biochimica et Biophysica Acta (BBA) - molecular. Cell Res. 1863, 2333–2344.

Ceccaldi, R., Rondinelli, B., D'Andrea, A.D., 2016. Repair pathway choices and consequences at the double-Strand break. Trends Cell Biol. 26, 52–64.

Chang, X.-J., Zheng, C.-Q., Wang, Y.-W., Meng, C., Xie, X.-L., Liu, H.-P., 2016. Differential protein expression using proteomics from a crustacean brine shrimp (*Artemia sinica*) under CO2-driven seawater acidification. Fish Shellfish Immunol. 58, 669–677.

Clement, K., Rees, H., Canver, M.C., Gehrke, J.M., Farouni, R., Hsu, J.Y., Pinello, L., 2019. CRISPResso2 provides accurate and rapid genome editing sequence analysis. Nat. Biotechnol. 37, 224–226.

Davis, A.J., Chen, D.J., 2013. DNA double strand break repair via non-homologous end-joining. Transl. Cancer Res. 2, 130–143.

Edvardsen, R.B., Leininger, S., Kleppe, L., Skaftnesmo, K.O., Wargelius, A., 2014. Targeted mutagenesis in Atlantic Salmon (*Salmo salar L.*) using the CRISPR/Cas9 system induces complete knockout individuals in the F0 generation. PLoS One 9, e108622.

FAO, 2020. The State of World Fisheries and Aquaculture 2020. Sustainability in Action. FAO, Rome.

Furuhashi, M., Morimoto, Y., Shima, A., Nakamura, F., Ishikawa, H., Takeuchi, S., 2021. Formation of contractile 3D bovine muscle tissue for construction of millimetre-thick cultured steak. NPJ Sci. Food. 5, 6.

Gao, Y., Zhang, X., Zhang, X., Yuan, J., Xiang, J., Li, F., 2020. CRISPR/Cas9-mediated mutation reveals Pax6 is essential for development of the compound eye in Decapoda *Exopalaemon carinicauda*. Dev. Biol. 465, 157–167.

Gratacap, R.L., Wargelius, A., Edvardsen, R.B., Houston, R.D., 2019. Potential of genome editing to improve aquaculture breeding and production. Trends Genet. 35, 672–684.

Gui, T., Zhang, J., Song, F., Sun, Y., Xie, S., Yu, K., Xiang, J., 2016. CRISPR/Cas9-mediated genome editing and mutagenesis of *EcChi4* in *Exopalaemon carinicauda*. G3: Genes Genom Genet. 6, 3757–3764.

Hsu, Patrick D., Lander, Eric S., Zhang, F., 2014. Development and applications of CRISPR-cas9 for genome engineering. Cell. 157, 1262–1278.

Hu, X.F., Zhang, B., Liao, C.H., Zeng, Z.J., 2019. High-efficiency CRISPR/Cas9-mediated gene editing in honeybee (*Apis mellifera*) embryos. G3 Genes Genome Genet. 9, 1759–1766.

Hwang, W.Y., Fu, Y., Reyon, D., Maeder, M.L., Tsai, S.Q., Sander, J.D., Joung, J.K., 2013. Efficient genome editing in zebrafish using a CRISPR-Cas system. Nat. Biotechnol. 31, 227–229.

Jaganathan, D., Ramasamy, K., Sellamuthu, G., Jayabalan, S., Venkataraman, G., 2018. CRISPR for crop improvement: an update review. Front. Plant Sci. 9.

Jordan, T., Hanson, I., Zaletayev, D., Hodgson, S., Prosser, J., Seawright, A., van Heyningen, V., 1992. The human *PAX6* gene is mutated in two patients with aniridia. Nat. Genet. 1, 328–332.

Karplus, I., Barki, A., 2019. Male morphotypes and alternative mating tactics in freshwater prawns of the genus *Macrobrachium*: a review. Rev. Aquac. 11, 925–940.

Kim, J., Cho, J.Y., Kim, J.-W., Kim, H.-C., Noh, J.K., Kim, Y.-O., Kong, H.J., 2019. CRISPR/Cas9-mediated myostatin disruption enhances muscle mass in the olive flounder *Paralichthys olivaceus*. Aquaculture. 512, 734336.

Kishimoto, K., Washio, Y., Yoshiura, Y., Toyoda, A., Ueno, T., Fukuyama, H., Kinoshita, M., 2018. Production of a breed of red sea bream *Pagrus major* with an increase of skeletal muscle mass and reduced body length by genome editing with CRISPR/Cas9. Aquaculture. 495, 415–427.

Klann, M., Seaver, E.C., 2019. Functional role of *Pax6* during eye and nervous system development in the annelid *Capitella teleta*. Dev. Biol. 456, 86–103.

Kumagai, H., Nakanishi, T., Matsuura, T., Kato, Y., Watanabe, H., 2017. CRISPR/Cas-mediated knock-in via non-homologous end-joining in the crustacean *Daphnia magna*. PLoS One 12, e0186112.

Levy, T., Rosen, O., Eilam, B., Azulay, D., Aflalo, E.D., Manor, R., Sagi, A., 2016. A single injection of hypertrophied androgenic gland cells produces all-female aquaculture. Mar. Biotechnol. 18, 554–563.

Levy, T., Tamone, S.L., Manor, R., Bower, E.D., Sagi, A., 2020. The protandric life history of the northern spot shrimp *Pandalus platyceros*: molecular insights and implications for fishery management. Sci. Rep. 10, 1287.

Ling, S.W., 1969a. The general biology and development of *Macrobrachium rosenbergii* (DE MAN). FAO Fish. Rep. 3.

Ling, S.W., 1969b. The general biology and development of *Macrobrachium rosenbergii* (DE MAN). FAO Fish. Rep. 3.

Lino, C.A., Harper, J.C., Carney, J.P., Timlin, J.A., 2018. Delivering CRISPR: a review of the challenges and approaches. Drug Deliv. 25, 1234–1257.

Liu, W., Xie, Y., Ma, J., Luo, X., Nie, P., Zuo, Z., Ren, J., 2015. IBS: an illustrator for the presentation and visualization of biological sequences. Bioinformatics. 31, 3359–3361.

Ma, J., Zeng, L., Lu, Y., 2017. Penaeid shrimp cell culture and its applications. Rev. Aquac. 9, 88–98.

Maekawa, S., Nishida, E., Ohta, Y., Sakai, H., 1984. Isolation of low molecular weight actin-binding proteins from porcine brain 1. J. Biochem. 95, 377–385.

Martin, A., Serano, Julia M., Jarvis, E., Bruce, Heather S., Wang, J., Ray, S., Patel, Nipam H., 2016. CRISPR/Cas9 mutagenesis reveals versatile roles of hox genes in crustacean limb specification and evolution. Curr. Biol. 26, 14–26.

Minelli, A., Boxshall, G., Fusco, G., 2016. Arthropod Biology and Evolution. Springer.

Okoli, A.S., Blix, T., Myhr, A.I., Xu, W., Xu, X., 2021. Sustainable use of CRISPR/Cas in fish aquaculture: the biosafety perspective. Transgenic Res. 31, 1–21. https://doi.org/10.1007/s11248-021-00274-7.

Pillai, B.R., Lalrinsanga, P.L., Ponzoni, R.W., Khaw, H.L., Mahapatra, K.D., Sahu, S., Pradhan, H., 2020. Selective breeding of giant freshwater prawn (*Macrobrachium rosenbergii*) in India: response to selection for harvest body weight and on-farm performance evaluation. Aquac. Res. 51, 4874–4880.

Rotem-Dai, N., Weil, S., Greenshpan, Y., Abehsera, S., Manor, R., Ofir, R., Sagi, A., 2021. Lentiviral-transduced ectopic expression of androgenic hormone in a crustacean hematopoietic primary cell culture. Frontiers in marine. Science. 8.

Rubio, N., Datar, I., Stachura, D., Kaplan, D., Krueger, K., 2019. Cell-based fish: a novel approach to seafood production and an opportunity for cellular agriculture. Front. Sustain. Food Syst. 3.

Scheufele, D.A., Krause, N.M., Freiling, I., Brossard, D., 2021. What we know about effective public engagement on CRISPR and beyond. Proc. Natl. Acad. Sci. 118, e2004835117.

Sternberg, S.H., Redding, S., Jinek, M., Greene, E.C., Doudna, J.A., 2014. DNA interrogation by the CRISPR RNA-guided endonuclease Cas9. Nature. 507, 62–67.

Tuladhar, R., Yeu, Y., Tyler Piazza, J., Tan, Z., Rene Clemenceau, J., Wu, X., Lum, L., 2019. CRISPR-Cas9-based mutagenesis frequently provokes on-target mRNA misregulation. Nat. Commun. 10, 4056.

Turnbull, C., Lillemo, M., Hvoslef-Eide, T.A.K., 2021. Global regulation of genetically modified crops amid the gene edited crop boom – a review. Front. Plant Sci. 12.

Wilson, L.O.W., O'Brien, A.R., Bauer, D.C., 2018. The current state and future of CRISPR-Cas9 gRNA design tools. Front. Pharmacol. 9.
Wu, P., Qi, D., Chen, L., Zhang, H., Zhang, X., Guang Qin, J., Hu, S., 2009. Gene discovery from an ovary cDNA library of oriental river prawn *Macrobrachium nipponense* by ESTs annotation. Comp. Biochem. Physiol. Part D: Genom. Proteom. 4, 111–120.
Xu, S., Pham, T.P., Neupane, S., 2020. Delivery methods for CRISPR/Cas9 gene editing in crustaceans. Mar. Life Sci. Technol. 2, 1–5.